

Mathematical principles and models of plant growth mechanics

Smithers, Euan; Luo, Jingxi; Dyson, Rosemary

DOI:

[10.1093/jxb/erz253](https://doi.org/10.1093/jxb/erz253)

License:

Other (please specify with Rights Statement)

Document Version

Peer reviewed version

Citation for published version (Harvard):

Smithers, E, Luo, J & Dyson, R 2019, 'Mathematical principles and models of plant growth mechanics: from cell wall dynamics to tissue morphogenesis', *Journal of Experimental Botany*, vol. 70, no. 14, pp. 3587–3600. <https://doi.org/10.1093/jxb/erz253>

[Link to publication on Research at Birmingham portal](#)

Publisher Rights Statement:

This is a pre-copyedited, author-produced version of an article accepted for publication in *Journal of Experimental Botany* following peer review. The version of record Euan T Smithers, Jingxi Luo, Rosemary J Dyson, 'Mathematical principles and models of plant growth mechanics: from cell wall dynamics to tissue morphogenesis', *Journal of Experimental Botany*, Volume 70, Issue 14, 1 July 2019, Pages 3587–3600, is available online at: <https://doi.org/10.1093/jxb/erz253> and <https://academic.oup.com/jxb/article/70/14/3587/5498733>

General rights

Unless a licence is specified above, all rights (including copyright and moral rights) in this document are retained by the authors and/or the copyright holders. The express permission of the copyright holder must be obtained for any use of this material other than for purposes permitted by law.

- Users may freely distribute the URL that is used to identify this publication.
- Users may download and/or print one copy of the publication from the University of Birmingham research portal for the purpose of private study or non-commercial research.
- User may use extracts from the document in line with the concept of 'fair dealing' under the Copyright, Designs and Patents Act 1988 (?)
- Users may not further distribute the material nor use it for the purposes of commercial gain.

Where a licence is displayed above, please note the terms and conditions of the licence govern your use of this document.

When citing, please reference the published version.

Take down policy

While the University of Birmingham exercises care and attention in making items available there are rare occasions when an item has been uploaded in error or has been deemed to be commercially or otherwise sensitive.

If you believe that this is the case for this document, please contact UBIRA@lists.bham.ac.uk providing details and we will remove access to the work immediately and investigate.

1 Mathematical principles and models of plant growth
2 mechanics: from cell wall dynamics to tissue
3 morphogenesis

4 E.T. Smithers, J. Luo, R.J. Dyson

5
6 16th May 2019

7
8 E.T.Smithers:ets796@bham.ac.uk

9 J. Luo: J.Luo.5@bham.ac.uk

10 R.J.Dyson: R.J.Dyson@bham.ac.uk

11
12 Institution: The University of Birmingham

13 Address: Watson Building

14 University of Birmingham

15 Edgbaston

16 Birmingham B15 2TT

17 United Kingdom

18 Corresponding author telephone: 0121 4143415

19
20 6 Figures

21 Word count: 8163

22
23 Highlight (fewer than 30 words)

24 We explain the principles behind mathematical models of plant growth
25 mechanics and the biological insights they provide. We suggest open
26 questions for mathematicians and biologists to tackle in the future.

27 Abstract (max 200 words)

28 Plant growth research produces a catalogue of complex open questions. We argue that plant
29 growth is a highly mechanical process, and that mathematics gives an underlying framework
30 with which to probe its fundamental unrevealed mechanisms. This review serves to illustrate
31 the biological insights afforded by mathematical modelling and demonstrate the breadth of
32 mathematically-rich problems available within plant sciences, thereby promoting a mutual
33 appreciation across the disciplines. On the one hand, we explain the general mathematical
34 principles behind mechanical growth models; on the other, we describe how modelling
35 addresses specific problems in microscale cell wall mechanics, tip growth, morphogenesis
36 and stress feedback. We conclude by identifying possible future directions for both biologists
37 and mathematicians, including as-yet unanswered questions within various topics, stressing
38 that interdisciplinary collaboration is vital for tackling the challenge of understanding plant
39 growth mechanics.

40

41

42 Keywords (6-8 words)

43 Mechanics, modelling, growth, morphogenesis, pollen tubes, shoot apical
44 meristem, microtubules

45

46 1 Introduction

47

48 Plant growth is a highly mechanical process, incorporating both reversible (elastic) and
49 irreversible (plastic/viscoelastic) deformations. The cell wall withstands great tension,
50 equivalent to 100-1000 atmospheres of tensile stress (Cosgrove 2005), and consists of three
51 main components: cellulose, hemicellulose (e.g arabinoxylan or xyloglucan) and pectin
52 (Scheller and Ulvskov 2010, Höfte et al. 2012, Park and Cosgrove 2015, Jarvis 2009,
53 Cosgrove 2014). A cell wall inflated under the action of turgor pressure (causing wall stress)
54 will be stretched to mechanical equilibrium, exhibiting a constant elastic strain or
55 deformation. For growth to occur, there must be an irreversible deformation, which begins
56 when the mechanical load exceeds some critical value (yield). Growth is carefully mediated

57 via active control of the wall's mechanical properties (e.g. by enzymatic action or new
58 material deposition), altering either the yield or the post-yield behaviour

59

60 Growth is inherently a multiscale process, from rearrangement of the cell wall microstructure
61 to the behaviour of a whole tissue (figure 1). On the microscale, bond breakage and polymer
62 network rearrangement (wall loosening) results in a relaxation of wall stress, allowing for
63 viscous flow of the cell wall, whilst thinning of the wall can be balanced by deposition of
64 wall material. Drawing water into the cell during extension allows for permanent volume
65 increase (plastic growth) and maintains a high level of turgor. Wall loosening can be
66 mediated by the action of proteins or enzymes, such as expansins, xyloglucan
67 endotransglucosylase/hydrolase (XTH), pectin-modifying enzymes (PME) and/or regulated
68 by the action of hormones, such as auxin, gibberellins, abscisic acid, and so on (Cosgrove
69 2005, 2016). Turgor acts in all directions simultaneously as an isotropic force. To achieve
70 directional growth, cell walls can be mechanically anisotropic; this anisotropy is often
71 induced by the alignment of cellulose, thus cell walls highly regulate the direction of growth
72 (Baskin and Jensen 2013, Kierzkowski and Routier-Kierzkowska 2019). On the macroscale,
73 plant cells are rigidly connected to one another through their cell walls (unlike animal cells);
74 no slippage can occur. As a result, macroscale morphogenesis and growth must be a
75 collaborative process across the whole tissue (Hamant and Haswell 2017).

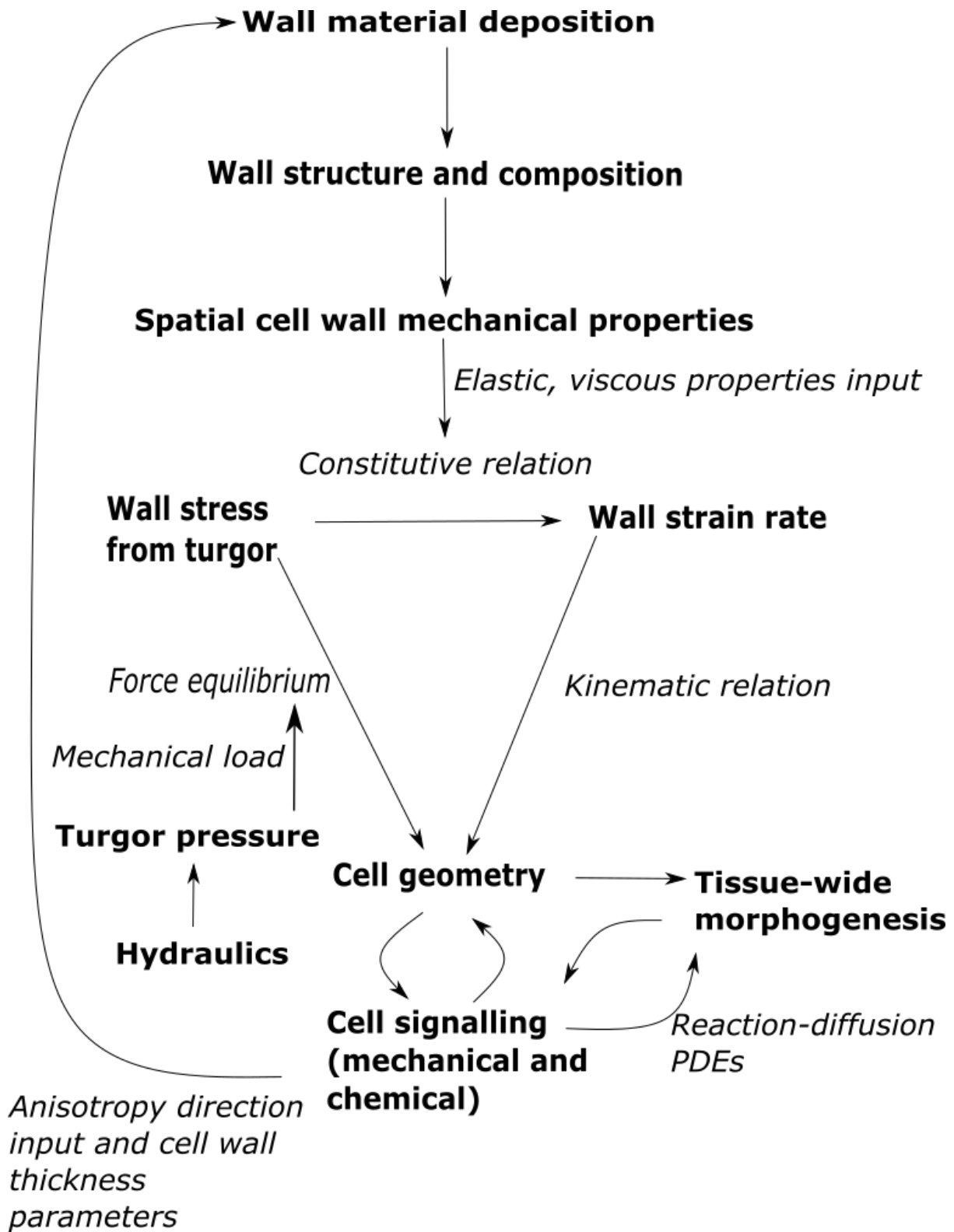
76

77 Existing reviews which examine the principles of plant growth mechanics include Geitmann
78 and Dyson (2013), Geitmann and Ortega (2009), Prusinkiewicz (2004) and Bruce (2003).
79 Chebli and Geitmann (2007) review specifically the mechanics of pollen tube growth.
80 Kierzkowski and Routier-Kierzkowska (2019) highlight the role of geometry in plant growth,
81 citing studies which incorporate imaging approaches. Hamant and Haswell (2017) summarise
82 the role of mechanical cues. Ali et al. (2014) and Chickarmane et al. (2010) both examine
83 morphogenesis, the latter specifically looking at the use of computational modelling.
84 Experimental procedures for quantifying mechanical behaviour have also been reviewed by
85 Bidhendi and Geitmann (2019), including discussion of how mathematics can aid in this
86 quantification.

87

88 There can be a lack of mutual appreciation between biologists and mathematicians about their
89 respective disciplines. Papers in biological journals receive 28% fewer citations for each
90 additional equation per page in the main article (Fawcett and Higginson 2012). This hinders

91 communication between researchers of different backgrounds. In this review we hope to
92 tackle this issue by highlighting the crucial biological insights which are generated through
93 mathematical models, in a way that readers who are unfamiliar with the underlying theory
94 can appreciate. We lay out an argument that mechanics is fundamental to plant growth and
95 morphogenesis, and that mathematical frameworks are required to describe the mechanistic
96 processes. Such frameworks allow access to details that experiments cannot determine
97 (Chickarmane et al. 2010), can bypass the practical challenges of experimentation on living
98 tissue (Dupuy et al. 2007), and provide a means of testing whether proposed mechanisms are
99 sufficient to explain observed behaviour. We begin our review by explaining in section 2 the
100 mathematical frameworks that underlie various plant growth models. In section 3, we dissect
101 mathematical models concerning a number of plant systems, ending each subsection with an
102 overview of the main ideas and future outlook. We finish the review by describing in sections
103 4 and 5 some prospective future directions for the field in general, including both biological
104 and mathematical questions.



105

106

107 Figure 1: Various aspects of growth mechanics (bold) connected by mathematical modelling

108 concepts (in italics), inspired by Dumais et al. (2006)

109

110 2 Mathematical Principles

111

112 Here, we introduce the mathematical principles which underlie the models described in
113 section 3. We give brief overviews of different classes of methodology, aiming to explain the
114 basic concepts only; references are given for more details on each technique. Key
115 words/concepts are indicated in italics, whilst interactions between concepts are summarised
116 in Figure 1.

117

118 Any mechanical model of a material (e.g. solid or fluid) is a set of mathematical equations
119 which relate the material’s intrinsic variables (including but not limited to deformations, flow
120 rates, potential energies and heat fluxes) to internal and external forces. Those equations
121 contain any number of *parameters*, which describe properties of the material. A parameter
122 can be *geometric*, meaning it involves dimensions of length only, such as an area or volume;
123 *kinematic*, involving dimensions of length and time, such as diffusivity; *dynamic*, involving
124 length, time and mass, such as Young’s modulus; or *thermodynamic*, involving length, time,
125 mass and temperature, such as heat capacity. The algebraic procedure of *non-*
126 *dimensionalisation* creates *dimensionless* parameters from suitable combinations of the
127 aforementioned dimensional ones, and uses scaling factors to remove dimensions (i.e. units)
128 from variables. Examples of dimensionless parameters include aspect ratios, efficiencies, and
129 Reynold’s number which is vital in many models of fluid flow. Expressing a mechanical
130 model in terms of dimensionless variables and parameters usually affords valuable insights
131 into the physical system, as the absence of “sizes” in the model implies that its outputs will
132 hold irrespective of sizes in the system. An exemplary explanation of non-dimensionalisation
133 can be found in Edelstein-Keshet (2005).

134

135 A primary example of a mechanical model of plant growth is the Lockhart equation
136 (Lockhart 1965):

$$\begin{aligned} 137 \quad \frac{1}{V} \frac{dV}{dt} &= \Phi_0(P - Y) \text{ if } P \geq Y \text{ and} \\ 138 \quad \frac{1}{V} \frac{dV}{dt} &= 0 \text{ if } P < Y, \end{aligned} \quad (1)$$

139 where V is the volume of a growing cell, t is time, P is turgor pressure within the cell, the
140 parameter Y is a turgor yield threshold below which no growth occurs, and Φ_0 is an

141 extensibility parameter. Despite its shortcomings, variations on the Lockhart equation have
142 become a standard paradigm for plant cell and tissue growth, as we discuss in section 3.

143

144 2.1 Continuum mechanics

145 Mechanical modelling of a material cannot be achieved at the scale of individual particles
146 such as electrons and atoms, for two reasons. Firstly, the vast number of particles involved
147 would make calculations practically impossible; secondly and more fundamentally,
148 behaviours of a material at the macroscale are emergent phenomena which, despite being
149 caused by collective interactions between particles, cannot be predicted from those
150 interactions (Anderson 1972). A well-developed theoretical framework, which bypasses
151 particle interactions and models a material as an infinitely divisible medium, is that of
152 continuum mechanics.

153

154 Every material must obey the ‘four fundamental axioms of mechanics’, each of which is a
155 *balance equation*, relating the rate of change of a variable – specifically mass, momentum
156 (mass \times velocity), angular momentum (mass \times orbital radius squared \times angular velocity), or
157 energy – to the internal and external influences that could cause such a change (Eringen
158 1980). *Reaction-diffusion* equations are an important type of balance equation, which
159 determine how the concentrations of quantities vary in time and space. In the biological
160 context, many cell growth models involve a reaction-diffusion component which governs the
161 dynamics of certain chemicals (e.g. pollen tube growth, section 3.2). If a continuum model is
162 *thermodynamic*, i.e. involving some flux of heat, then an additional, fifth axiom of mechanics
163 must be obeyed; this is the balance of entropy (Sandler 1999). An entropy balance equation
164 relates the rate of change of disorder in a physical system to heat transferred and/or
165 mechanical work done by the system. In some models of cell wall mechanics,
166 thermodynamic principles are used to determined energetically favourable wall structures
167 (e.g. micromechanics of cell wall construction, section 3.1).

168

169 As well as the universal balance equations, a mechanical model must include *dynamical*
170 *equations* which are specific to the material. A typical dynamical equation is the *constitutive*
171 *law*, relating a material’s *stress* (internal forces) to its *deformation* (extension) (Astarita and
172 Marrucci 1974, Paolucci 2016). The simplest constitutive law is Hooke’s law: force is
173 proportional to extension, with the constant of proportionality denoted by Young’s modulus,

174 also known as the spring constant (see figure 2(a)). Some models of tissue-wide growth
175 phenomena involve variations of Hooke's Law (e.g. the shoot apical meristem, section 3.3).
176 In general, a constitutive law describes the mechanical behaviour of the given material (is the
177 material solid/fluid, hard/soft, does it display any directional dependence, etc.). Most balance
178 and dynamical equations are mathematical entities known as *partial differential equations*
179 (PDEs). For a good introduction to PDEs, and examples rooted in real-world problems, we
180 refer the reader to Mattheij et al. (2005).

181

182 Broadly speaking, the two types of material with which we are concerned are *solids* and
183 *fluids* (more specifically, liquid fluids, as gaseous fluids are beyond the scope of this review).
184 The difference between them is clearly reflected in the constitutive law which, for a solid,
185 relates stress to *strain*, i.e. the amount of deformation, via a material property known as
186 *stiffness*; in contrast, the constitutive law for a fluid relates stress to strain-rate, i.e. the
187 velocity at which deformation occurs, via a property of the fluid called *viscosity*. For an
188 illustration of the various concepts we have introduced, see figure 2. However, the
189 categorisation of materials is far from binary. For instance, *viscoelastic* materials are
190 considered intermediate between solids and fluids, with constitutive laws relating stress to a
191 combination of strain and strain-rate (Dill 2007). Mathematical models of plant growth
192 require a choice of constitutive law appropriate to capture the key behaviour for a given
193 system on the time and length scales of interest (for example treating the cell wall as a
194 viscous fluid on a long timescale (see section 3.1).

195

196 Stress, strain and strain-rate in a material are represented mathematically by quantities known
197 as *tensors*. A tensor is written as an array of numbers and/or functions, with each entry
198 known as a *tensor* component. A rank-1 tensor is commonly known as a vector, whilst a
199 rank-2 tensor can be represented by a matrix. In 3-dimensional space, a vector has 3
200 components, and a rank-2 tensor – the most common type in continuum mechanics – has
201 $3^2=9$ components. In a stress tensor, each of the 9 components can be interpreted as stress in a
202 particular direction, such as normal stress (due to forces perpendicular to material cross-
203 sections) or shear stress (due to forces parallel to material cross-sections). Of particular note
204 in plant biomechanics are those stress tensors that display *anisotropy*, i.e. directional
205 variations. This type of stress is related to the geometry of cells (figure 1). For instance,
206 within spherical shapes the stress in the cell wall created by turgor tends to be isotropic (same
207 in every directions) but in elongated cells the stress is anisotropic, which is why cells need to

208 have circumferential cellulose reinforcement to resist the stress. Moreover, stress distribution
209 depends on morphology, in the sense that areas of reduced stress correspond to elongation
210 (Kierzkowski and Routier-Kierzkowska 2019, Kierzkowski et al. 2012). A practical, physics-
211 oriented description of generic tensors is contained in Arfken and Weber (1995), while the
212 technically-minded reader may enjoy the rigorous treatment of tensor algebra in Renteln
213 (2014) from the perspective of differential geometry. Specificities of stress, strain, strain-rate
214 and viscosity tensors are excellently elucidated in Spencer (2004).

215

216 We can roughly sub-categorise solids into elastic (whose deformations are entirely reversible)
217 and plastic (which exhibits irreversible deformation), and fluids into Newtonian (“normal”
218 fluids such as water) and non-Newtonian (“weird” fluids such as custard). For a Newtonian
219 fluid (which is assumed to be incompressible, i.e. with constant density), there is a simple
220 linear relation between stress and strain-rate, with the constant of proportionality being the
221 fluid viscosity, a measure of how much the fluid resists flow (see figure 2(b)). When a non-
222 Newtonian fluid is considered, stress and strain-rate may be related by a viscosity tensor,
223 giving a non-linear relationship (Brujan 2011). For a model to describe growth, irreversible
224 deformation must be possible; when a plant cell wall is modelled as a fluid, it is typically
225 non-Newtonian (see section 3.1); For solids, there exist numerous types of elasticity and
226 plasticity, each requiring its own model, which Spencer (2004) outlines succinctly. Each
227 model involves a strain energy function, which is differentiated to give the stress tensor.
228 When deformations are small, so that a linear relationship between stress and strain is found,
229 the solid is said to be linear elastic; for large deformations, the solid is hyperelastic. For
230 examples of hyperelastic models with sophisticated constitutive laws, such as the neo-
231 Hookean, Mooney-Rivlin, and Ogden models - the latter of which is particularly applicable to
232 biological tissue - the reader is referred to the comprehensive text by Ogden (2013). There is
233 a broad literature on the subjects of solids and fluids: Goodier and Hodge (1958) includes a
234 rich catalogue of solid mechanics problems; Parker (2003) is a clear, elementary account of
235 Newtonian fluids; and Brujan (2011) concisely explains the basic concept of non-Newtonian
236 fluids, giving examples of constitutive laws from various well-known models. For an in-
237 depth exposition of the vast number of non-Newtonian fluid models that exist, see Bird et al.
238 (1987).

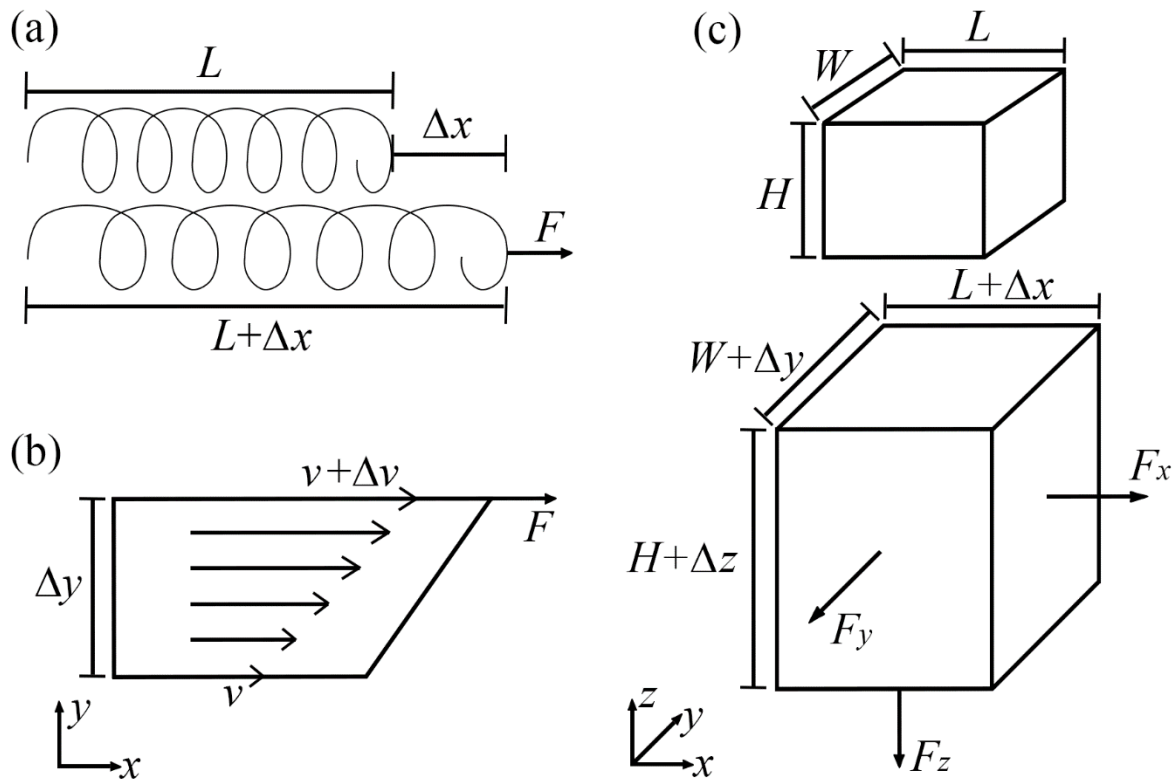


Figure 2. Stress, strain, and strain-rate. (a) The stretching and compressing deformation of a spring under an applied force is considered a one-dimensional system. Under the force F , the spring is in equilibrium (held at constant length), having extended from its natural length of L to its deformed length of $L+\Delta x$. To say the spring obeys Hooke's law means that there is some constant k , called the spring's *stiffness* (or spring constant), such that $F = k \Delta x$. An equilibrium state with twice the force will exhibit twice the extension, halving the force halves the extension, and so on. (b) The strain-rate (velocity) of an (infinitesimal volume of) Newtonian fluid, side-view. If the fluid flow is uniform in the z -direction (out of page), then the system is two-dimensional in (x,y) . The bottom plate flows at velocity v while the top plate, separated from the bottom by a distance Δy , flows at velocity $v+\Delta v$. The *shear stress* τ , defined as the shearing force F per unit area of the top plate, is related to Δy and Δv via a constant parameter called the fluid's *viscosity* μ : $\tau = \mu \Delta v / \Delta y$. (c) The strain (deformation) of an elastic solid under applied forces. The force on each surface is normal (perpendicular) to that surface, causing a strain according to a generalised Hooke's law: the vector (F_x, F_y, F_z) is related to the vector $(\Delta x, \Delta y, \Delta z)$ via some *stiffness matrix* with constant coefficients. If the force on any surface is not normal to that surface, then it will cause a shearing deformation. For example, if the force on the rightmost surface can be resolved into F_x along the x -axis and F_{xy} along the y -axis, then F_{xy} will cause a shear in the x - y plane. Components of the stress tensor are related to the (per-unit-area) forces, $F_x, F_y, F_z, F_{xy}, F_{yz}, F_{zx}$ (at equilibrium, $F_{xy} = F_{yx}$ etc.). For further mathematical details concerning the stress tensor, as well as the analogous strain tensor and strain-rate tensor, we refer the reader to Spencer (2004).

240 2.2 Asymptotics

241 PDEs in continuum mechanics models rarely admit exact solutions; in most situations,
242 approximate solutions are sought. One of the most commonly used techniques for finding
243 approximate solutions to a PDE is that of *asymptotics*. This method relies on the existence in
244 the system of a dimensionless parameter, say ϵ , whose value is ‘small’. For example, ϵ might
245 represent the ratio of cell wall thickness to cell length, or the ratio of some cross-sectional
246 area to surface area. One may then assume that any variable, say T , can be written as a
247 regular asymptotic expansion in the form of $T = T_0 + \epsilon T_1 + \epsilon^2 T_2 + \dots$, where T_0 is known as
248 the 0th-order solution and $T_{j>0}$ is known as the j^{th} -order correction. By substituting the
249 asymptotic expansion into the system, one may determine $T_{j \geq 0}$ in succession; including
250 higher-order corrections generally makes the solution more accurate. Steinrück (2010)
251 formalises the general principles of asymptotics that we have described, and provides
252 advanced examples. Further examples, which require the advanced method of matched
253 asymptotics, are presented in Kevorkian (2000). For an interesting historical note on the
254 development of asymptotic methods, we refer the reader to O’Malley (2014).

255

256

257 2.3 Finite elements

258 While *analytical* methods such as asymptotics are valuable in sufficiently simple systems,
259 more complicated systems may require a *numerical* approach. The method of finite elements
260 is a popular one for solving continuum mechanics models over a finite domain. The basis of
261 the method is to partition the domain, such as the cell wall of a pollen tube, into a number of
262 appropriately defined, usually small, regions called finite elements. One then looks for an
263 approximate global solution which is represented within each element by a simple function.
264 When the domain is a plant tissue, cells can be represented as vertices interconnected by
265 edges representing cell walls; these edges are typically modelled as springs with some
266 prescribed mechanical behaviour. This type of finite-element modelling approach is known as
267 the *vertex element method* and will be explained further in section 3.3.

268

269 In Evans et al. (2000), the reader will find a detailed and practical introduction to finite-
270 element methods, with worked examples that demonstrate solving some well-known physical
271 problems. Elman et al. (2005) describes fast finite-element algorithms which are suited
272 specifically to equations of fluid mechanics. A recent review by Bidhendia and Geitmann

273 (2018) offers a critical analysis of the use of FE methods in mechanical plant cell modelling,
274 and advocates the use of FE for various plant growth problems, provided that good modelling
275 practice is followed.

276

277 3 Models of Growth Mechanics

278

279 In this section, we summarise the insights into some plant growth scenarios provided by
280 mathematical modelling techniques. Where appropriate, we explain how the models have
281 been derived and solved. Beginning with the microscale and cellular aspects of growth in
282 section 3.1, we review how cell wall components hold stress and how they are arranged. In
283 section 3.2 we give an overview of models of tip-growing cells, specifically pollen tubes.
284 This is followed by section 3.3, where we look at models on a larger scale, which deal with
285 the mechanical process in morphogenesis, specifically in pavement cells and shoot apical
286 meristem (SAM), and tissue signalling (thus following the flow of figure 1 by starting at the
287 top and reading down).

288

289 We assume in this review that cellulose deposition angle is highly influenced by
290 microtubules; even though it has been shown that this is not necessarily the case, and there is
291 ongoing debate about the regulatory effect of microtubules on cellulose alignment and
292 anisotropy (Baskin 2005, Cosgrove 2014, Baskin 2001). We will expand on this issue in
293 Section 4. We will also be focusing only on the primary cell wall.

294

295 3.1 Cell wall properties and construction

296 Models of cellular and microscale dynamics within the cell wall may help to resolve the long-
297 standing apparent paradox that the wall is weak enough to yield under turgor, yet strong
298 enough for the cell to remain intact and resist bursting. The models described below
299 incorporate elements of the cell wall microstructure to determine the emergent growth
300 behaviour (see figure 1) and/or macroscale mechanical characteristics

301

302 It has been a matter of debate as to how cellulose fibres are connected within the cell wall.
303 This is an important question, as the links between cellulose microfibrils by matrix
304 polysaccharides determine most of the physical properties of the cell wall (Cosgrove 2005).

305 One early theory was the tethered/sticky network model, which assumed cellulose molecules
 306 were joined continuously along their lengths, and peel off as they get increasingly stretched
 307 during cell growth (Cosgrove 1993). There has been growing experimental evidence against
 308 this theory; for instance the observation that xyloglucan-digesting enzymes (xyloglucan is a
 309 hemicellulose that is said to crosslink the microfibrils) do not have a significant impact on the
 310 strength of the cell wall (Cosgrove 2014). According to a finite-element model featuring a
 311 network of cellulose molecules tethered together by hemicellulose via hydrogen bonds, a
 312 deformed network is not strong enough to withstand the strain (Yi and Puri 2012). This is
 313 evidence that the tethered network model is not a feasible explanation as to how the cell wall
 314 retains integrity. A plausible alternative theory of cell wall connectivity is the biomechanical
 315 hotspot hypothesis, which suggests that wall extensibility is controlled by a limited number of
 316 cellulose-cellulose contacts, potentially coordinated by xyloglucan (Cosgrove 2014). One
 317 hotspot model considers a network of cellulose connected by hotspots represented as linear
 318 springs (Nili et al. 2015). The model implies that a group of short xyloglucan strands is stiffer
 319 than a single long strand, and it can produce the requisite wall stiffness to oppose turgor. The
 320 hotspot hypothesis also claims that a small amount of degradation of the hotspots could lead
 321 to the load being carried by pectin, which then enables viscous flow of the cell wall,
 322 providing a possible mechanism for growth.

323

324 The micromechanics of cell wall construction allows for controlled creep and determines the
 325 ability of the cell wall to withstand turgor pressure, but the exact roles of the different wall
 326 elements in strength and in wall loosening are still unknown (Park and Cosgrove 2015,
 327 Cosgrove 2014, Braybrook et al. 2012). The fibres may play different roles at different states
 328 of the cell wall. It has been suggested that pre-yield (low strain) dynamics of the cell wall are
 329 dominated by hemicellulose fibres stretching and breaking, while post-yield behaviour (high
 330 strain) is dominated by pectins (Dyson et al. 2012). This was investigated using a fluid
 331 mechanical model of the cell wall, considering growth as a fluid flow which drives the
 332 stretching/straining of a network of hemicellulose fibres, each represented by a spring with
 333 stiffness κ , rest-length L_0 , and evolving length L which is a function of time. These fibres
 334 connect cellulose molecules, with a breakage rate depending on the current strain. The stress
 335 resultant, Σ (essentially the axial tension), of the cell wall is found by summing (integrating)
 336 the effect of all bonds across the wall thickness, giving

$$\Sigma = \int_0^h n\kappa(L - L_0) dy + \frac{\alpha}{\phi_M}, \quad (2)$$

337

338 where h is the thickness of the cell wall, n the density of hemicellulose bonds, y the
339 coordinate across the wall thickness, α the strain (growth) rate, and α/ϕ_M represents the
340 contribution of pectin. The concentration of fibres might also affect wall strength. By re-
341 deriving the Lockhart equation from thermodynamic principles, it can be shown that the cell
342 wall yield is primarily determined by the concentration of xyloglucans and cellulose, and not
343 the bonds between them (Veytsman and Cosgrove 1998). Even though this model considers a
344 small time-scale on which material deposition is negligible, wall yield depends on xyloglucan
345 concentration which in turn is determined by wall deposition. This implies an influential role
346 of deposition in wall loosening and consequently in growth. The flexibility of the fibres also
347 influences cell wall stress because hemicellulose could be trapped within the cellulose fibres.
348 However, interactions with pectin are not incorporated within this framework.

349

350 The CMF is said to have a highly regulatory effect on extensibility and maintaining cell
351 shape, but the detailed consequences of reorientation, distribution and crosslinking during
352 growth are missing (Anderson et al 2010). Using linear elasticity under imposed turgor to
353 examine the impact of CMF orientation, it has been found that it affects the radial elastic
354 deformation at the ends of the cell, but that the presence of CMF on the cell end plates makes
355 little difference to the cell's axial expansion (Ptashnyk and Seguin 2016). The model predicts
356 that shifting the positions of the cells out of alignment in the tissue (i.e. lined up like bricks in
357 a wall) allows for larger strains and increases the effect of varying microfibril configurations
358 on axial expansion. A variety of orientations throughout the wall also reduces axial expansion
359 and slightly increases radial growth. Another model has also found that the cell radius is
360 maintained via the CMF (Dyson and Jensen 2010). Representing the cell wall as a fibre-
361 reinforced thin sheet of viscous fluid, this model includes fibres (representing the CMF)
362 which are convected by growth, and is analysed and solved using asymptotics. The model
363 also finds that a variety of fundamental geometric and mechanical parameters related to the
364 composite cell wall properties govern the cell wall extensibility.

365

366 Efforts have been made to understand pectins' regulatory effects on growth. Pectins are
367 known to form hydrated gels that can force microfibrils apart, allowing for wall extensibility
368 to increase and the microfibrils to slip (Cosgrove 2005). Deposition of pectin is also said to
369 play a role, although its significance is still not completely understood. Using thermodynamic
370 constitutive laws which involve turgor, temperature, volume, free and bound pectate, and the
371 synthesis of pectates, a growth rate that principally depend on pectate crosslink synthesis can

372 be derived (Barbacci et al. 2013) (see figure 3). The comparison of this model's predictions
373 with data concerning *Chara corallina* is "quite good". Meanwhile, by balancing cell wall
374 growth rate and pectin insertion rate, it has been argued that turgor-driven deposition leads to
375 cell wall polymerisation (see figure 3), which is a primary growth control mechanism (Ali
376 and Traas 2016). The insertion rate in the model is derived from the thermodynamics
377 principle of balancing the free energy difference between bound and unbound pectin states.
378 Although the results match data qualitatively to *Chara corallina*, the authors acknowledge
379 that other mechanisms are at play. Both of the pectin studies consider *Chara corallina* which
380 contain a high amount of pectin, so these results may not be generalisable. It seems that
381 hemicellulose connections do influence the yield threshold of growth, and these studies
382 emphasise the role of pectins insertion in the viscous flow of the cell wall.

383

384 There are still remaining mysteries in cellular and microscale growth. For instance, despite
385 growing evidence for the biomechanical hotspot hypothesis as we have described, there is no
386 universal consensus on how the cell wall polymers are connected. Moreover, most studies
387 heavily rely on xyloglucan being the load-bearing component in the cell wall, but it has been
388 noted that xyloglucan possibly covers only a small portion of cellulose surface in the onion
389 wall (Zheng et al. 2018), and that *Arabidopsis* mutants containing small amounts of
390 xyloglucan have only minor changes in growth phenotype (Cosgrove 2016). The exact role of
391 pectin in the cell wall structure has also not been carefully investigated. All of these are
392 prerequisites for understanding how the cell wall expands. There has also not been substantial
393 work on the action of enzymes. Some models have shown that in order to match experimental
394 data, expansin must affect extensibility (Pietruszka 2011). Apart from this, not much work
395 has been done to model how enzymes manipulate the cell wall to cause wall relaxation,
396 strengthening, etc., and we will expand on this point in section 4.

397

398 3.2 Tip-growing cells

399 There are a number of cells such as pollen tubes and root hairs which extend via tip growth,
400 where growth is highly localised to one area of the cell wall. Growth rates are typically very
401 high, despite turgor pressures similar to other cell types (Beauzamy et al. 2014). Tight control
402 of both mechanical properties and new material deposition is therefore required, and
403 modelling can help understand these coupled processes (Geitmann and Emons 2000). Here
404 we review tip growth in pollen tubes.

405

406 Pollen tubes are of particular interest due to their high growth rate (1cm/h) (Bove et al. 2008)
407 and their oscillatory growth patterns (Kroeger and Geitmann 2012), but their growth is as yet
408 not fully understood. To model pollen tube growth, one needs to couple cell mechanics to
409 biochemical processes (Cameron and Geitmann 2018). Measurements of turgor do not show
410 significant oscillations, implying that it is likely not a driving mechanism behind growth
411 oscillations (Beauzamy et al. 2014). One possible explanation for oscillatory growth is a
412 vesicle recycling mechanism dependant on calcium concentration, where the fusion of
413 vesicles at the apex is stimulated by calcium ions (Kroeger et al. 2008). In this framework,
414 the pollen tube invading the external media is modelled as one viscous fluid being injected
415 into another, surrounded by a viscoelastic membrane representing the wall. The overall
416 growth velocity is calculated via Darcy's law of pressure-driven fluid flow

417
$$\mathbf{u} = \frac{K}{\mu} \nabla p, \quad (3)$$

418 where \mathbf{u} is the tip apex velocity, K denotes the permeability of the external medium, μ the
419 viscosity of the cell, p is the pressure, and ∇p gives the magnitude and direction of the
420 pressure gradient. The idea behind this model is that the rate of flow/growth is proportional to
421 the difference in pressure between two different regions (there is higher pressure in the cell
422 due to turgor which drives the flow outwards), similar to diffusion. An effective elastic
423 constant is incorporated into the fluid flow/growth rate, which in turn is dependent on
424 calcium concentration at the cell walls (see figure 3). The calcium exocytosis rate on the cell
425 wall is determined from a reaction-diffusion equation. These results agree qualitatively with
426 experimental observations, with some discrepancies due to calcium absorption by the cell
427 wall being neglected; this suggests that the assumption of calcium dynamics driving vesicle
428 recycling could be robust. The pollen tube growth phenomenon of pearled morphology
429 (oscillations in diameter to form a wavy boundary) is also not understood. A possible
430 explanation is that it occurs as a result of the extension and deposition rates being out of
431 phase (Rojas et al. 2011). Employing a principle that deposition causes crosslink turnover,
432 this model considers a computational lattice network of nodes which are connected if there is
433 a crosslink (modelled as linear springs), incorporating both esterified and de-esterified pectin
434 (see figure 3). The model predicts both steady and oscillatory growth, agreeing with
435 experimental data. Alternative morphologies have been observed in pollen tubes consisting of
436 swelling or tapering of the pollen tube head; unlike the causes above which both relate to
437 deposition, other mechanisms could be at play here. One model claims that the swelling

438 arises due to an insufficiently steep decrease in Young's modulus along the growth direction
 439 (Fayant et al. 2010). This claim is validated by the distribution of de-esterified (stiffer) pectin.
 440 The model also suggests that cellulose are important in resisting radial expansion, despite the
 441 randomness of their orientations. In conclusion, the model posits that the features affecting
 442 growth are spatially-varying components of the cell wall.

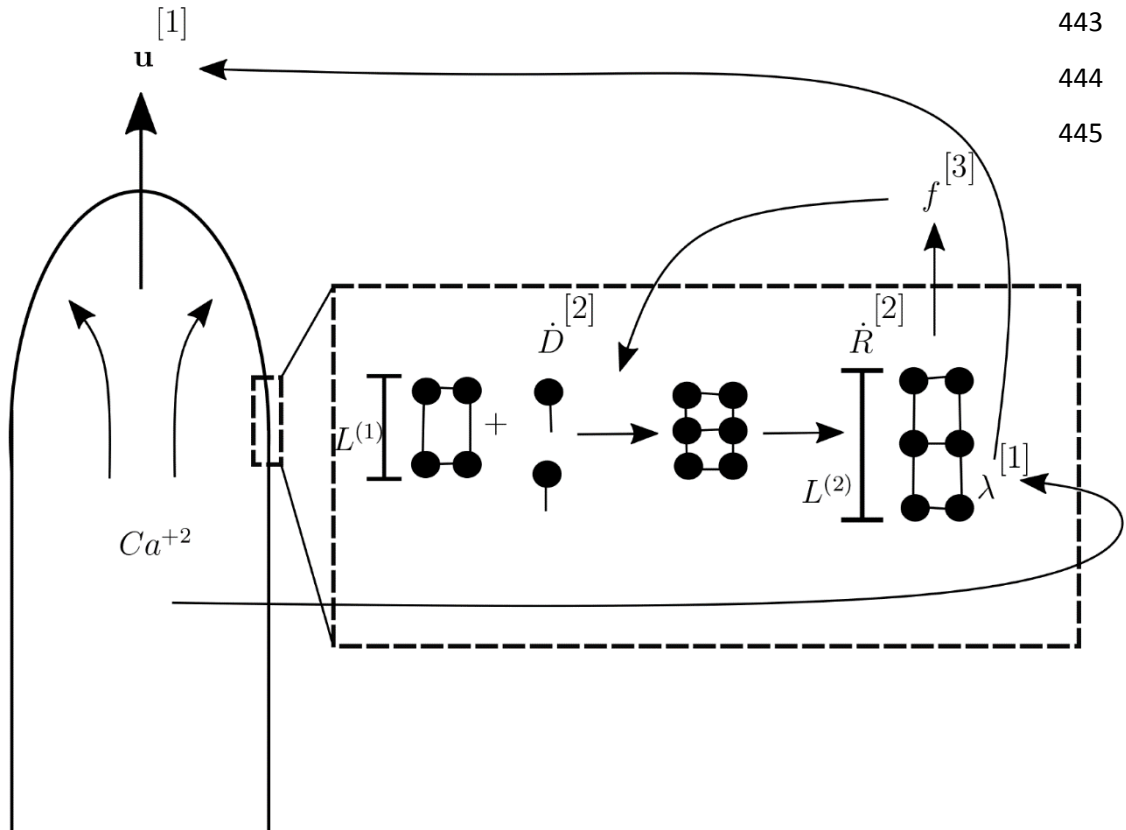


Figure 3: Pollen tube and pectin driven growth model principles. Kroeger et al. (2008) predict that the pressure gradient and calcium ion concentration both effect growth, \mathbf{u} (equation 3) with the former determining the direction and latter affecting the elasticity constant, λ which in turn affects the extension rate (labelled [1]). Rojas et al. (2011) assume the deposition of pectin with rate \dot{D} causes crosslink turnover, leading to extension in length from $L^{(1)}$ to $L^{(2)}$ with rate \dot{R} (labelled [2]). Note diagram depicts only demethylesterified pectin. This pectin deposition driven growth framework also demonstrates the modelling ideas behind Ali and Traas (2016) and Barbacci et al. (2013) in *Chara corallina* with the former model using turgor driven extension of the wall (denoted as f), driving further polymerisation (labelled [3]).

446 There remain unexplored territories within pollen tube modelling. Most models assume
 447 axisymmetric growth with a straight centreline (in order to reduce complexity and
 448 computational time), and therefore are unsuited for investigating complex mechanisms such
 449 as steering, which to our knowledge has not been explicitly modelled. Regarding oscillatory
 450 growth, there is evidence that calcium-ion oscillations occur in non-growing pollen tubes,
 451 showing it could be independent of growth (Cameron and Geitmann 2018), motivating

452 further work in this area.

453

454 3.3 Models of tissue growth

455 We turn our attention to larger-scale models which are evaluated across tissues, where
456 mechanics influences both shape and growth (see figure 1). Plant cells are tightly fixed to
457 each other, therefore growth and morphogenesis arise due to collaborative expansion, cell
458 division and communication between cells (Cosgrove 2005, Hamant and Haswell 2017,
459 Mirabet et al. 2011). For example, careful control of organ growth is observed in leaves with
460 a reduced cell number, which still reach normal size by increasing the rate or duration of their
461 cell expansion, demonstrating shape-sensing mechanisms (Hervieux et al. 2016). In this
462 section, we review mathematical insights into problems posed by pavement cells, shoot apical
463 meristems (SAM) and stress signalling.

464

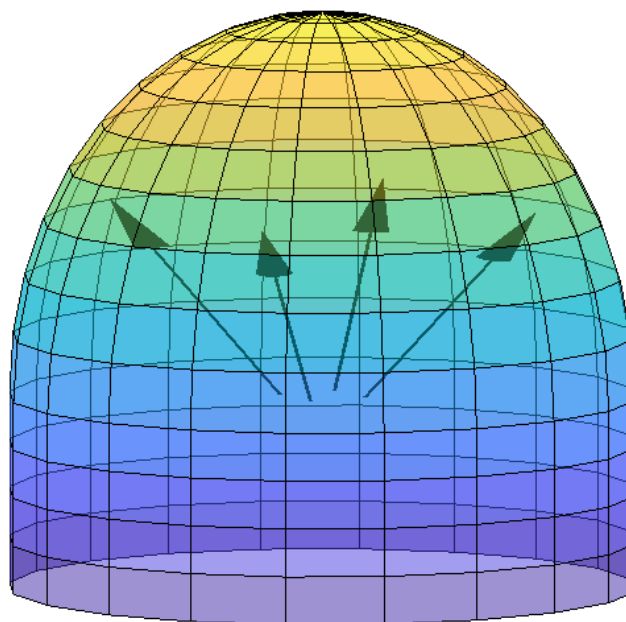


Figure 4: The concept of a shell model approximating a 3D tissue as a thin shell of epidermis inflated by pressure from the inner tissue. This significantly reduces computational time. The square objects on the shell represent a simple example mesh and do not correspond to cell walls.

465 We first explain the concept of a shell model. This is a 2D representation, a simplification of
466 the 3D tissue whereby only the outer epidermal layer is explicitly modelled, and tension from
467 the inner layers is imposed (see figure 4). The epidermis bears higher resistance to the
468 tension, as demonstrated experimentally. For example, a peeled, isolated epidermis will
469 contract, showing that it is under high stress (Savaldi-Goldstein et al. 2007, Hamant and

470 Haswell 2017, Beauzamy et al. 2015). Since the outer epidermis heavily restricts plant
471 growth, the 2D shell can be a realistic assumption.

472

473 The diversity of shapes of epidermal cells in leaves (pavement cells) is truly spectacular.
474 Some form highly undulating anticlinal walls, as in *Arabidopsis*, which lead to jigsaw-like
475 patterns of cells (Vöfely et al. 2018). Mechanical stress is said to play an important role in
476 determining these cells' geometry, but why and how the jigsaw patterns form has not been
477 elucidated (Sapala et al. 2019). Here we shall refer to the indents and protrusions of a
478 pavement cell as necks and lobes, respectively. Stress is found to be higher in the neck
479 regions, by extracting 3D cell shapes using MorphoGraphX (de Reuille et al. 2015) and
480 meshing the resulting surface, then incorporating fibre directions in a hyperelastic model
481 (Sampathkumar et al. 2014). Moreover, by considering idealised ellipsoidal cells with or
482 without protrusions, stress is found to transfer from the centres of cells to the neck regions,
483 consequently reducing the overall stress (Sapala et al. 2018). Since the spongy mesophyll
484 layer, which lies underneath the epidermis, contains air holes, it might not be able to provide
485 strength to the tissue, therefore the epidermis must withstand most of the total stress. Thus,
486 the stress reduction provided by the jigsaw morphology could be advantageous, as it could
487 help reduce the resources needed to strengthen the tissue and/or reduce the chance of the
488 tissue rupturing. As for *how* the jigsaw patterns come about, it has been shown that
489 microtubules align with the direction of maximal stress, which can then reinforce the necks
490 through the deposition of cellulose (Sampathkumar et al. 2014). The cellulose can then
491 restrict expansion at the necks, which in turn increases the stress, creating a feedback loop
492 where microtubules continue to align with the stress. This is a possible mechanism for how
493 the lobes become more prominent and enlarge, but it still does not answer how the lobes
494 *initially* form. To that end, a positive relationship between isotropic growth and 'lobeyness'
495 has been proposed (Sapala et al. 2018). The model is validated by a 2D simulation of cells,
496 where the walls are represented as nodes connected by linear springs (figure 6 – see
497 description later in this section), with additional intra-cell springs to represent stiffening
498 components such as cellulose.

499

500 It has also been suggested that lobe formation is a result of wall heterogeneities which cause
501 buckling when the leaf epidermis is under tension from variations in growth rates across
502 different cell layers (Majda et al. 2017). However, when this 2D modelling approach of only
503 including the anticlinal walls (wall perpendicular to leaf surface) was recreated, the lobe

504 amplitude was not as significant; including the effect of the periclinal walls (wall parallel to
505 leaf surface) the lobes are found to disappear (Bidhendi and Geitmann 2019). An alternative
506 model including the periclinal wall was developed using finite element methods assuming the
507 cell wall is neo-Hookean hyperelastic (Bidhendi et al. 2019). Upon analysis it was found that
508 varying periclinal wall stiffness between neighbouring cells can induce lobe formation; a
509 potential buckling mechanism is proposed due to cell geometry and internal pressure.
510 Reduction of stress is therefore most likely a factor in why pavement cells form these
511 interesting geometries but the origins of how they form could be connected with periclinal
512 wall mechanics and possible buckling.

513

514 The shoot apical meristem (SAM) has often been of interest to plant biologists, due to its
515 complex morphology of forming organ primordia, and because of its importance in leaf and
516 floral meristems and stem development (Soyars et al. 2016). The SAM must maintain a
517 source of undifferentiated cells, and differentiate cells in order to initiate organogenesis. This
518 requires strict co-ordination and structure, which are not yet understood (Truskina and
519 Vernoux 2018). The SAM's elastic and plastic properties which enable bulge initiation are
520 also a mystery. There surely must be varying properties in the region to allow for the
521 different growth rates in the shoot apex central zone and periphery. It has been proposed that
522 the slow-growing area at the shoot tip is significantly strain-stiffened, and this may control
523 the expansion process of the tip (Kierzkowski et al. 2012) (see figure 5). This model
524 concludes that the difference between tip and peripheral growth rates is not due to variations
525 in stress, but instead due to variations in other parameters such as yield threshold. In terms of
526 methodology, the model approximates the surface as a shell of Ogden hyperelastic material
527 (cf. section 2 and figure 4) with two regions of differing elastic properties: the shell tip where
528 stiffness increases with strain, and the periphery where stiffness is constant. Validation of the
529 model is provided by reproducing material behaviour from osmotic treatment experiments.
530 Differing regions of elastic properties are also echoed by another model, which tests different
531 mechanisms of organ emergence (Boudon et al. 2015). It finds that a bulge (similarly to the
532 above) could be produced by changing the stiffness of the outer cell layers near the bulge tip,
533 but not through variations in turgor or wall stiffness from interior layers. By creating a highly
534 rigid ring around the bulge of cells, to promote further growth, the model produces a more
535 distinct bump (see figure 5). This is a 3D model of tissue growth which includes gene
536 regulation, and a generalised Lockhart equation relating the plastic deformation tensor to the
537 elastic strain tensor. Both of the SAM models we have discussed illustrate the necessary

538 mechanical features to allow bulge initiation and maintain SAM morphogenesis, namely: in
539 order to adapt the stiffness properties, cell wall properties of the surrounding cells vary with
540 the distance from the tip of the initiation site.

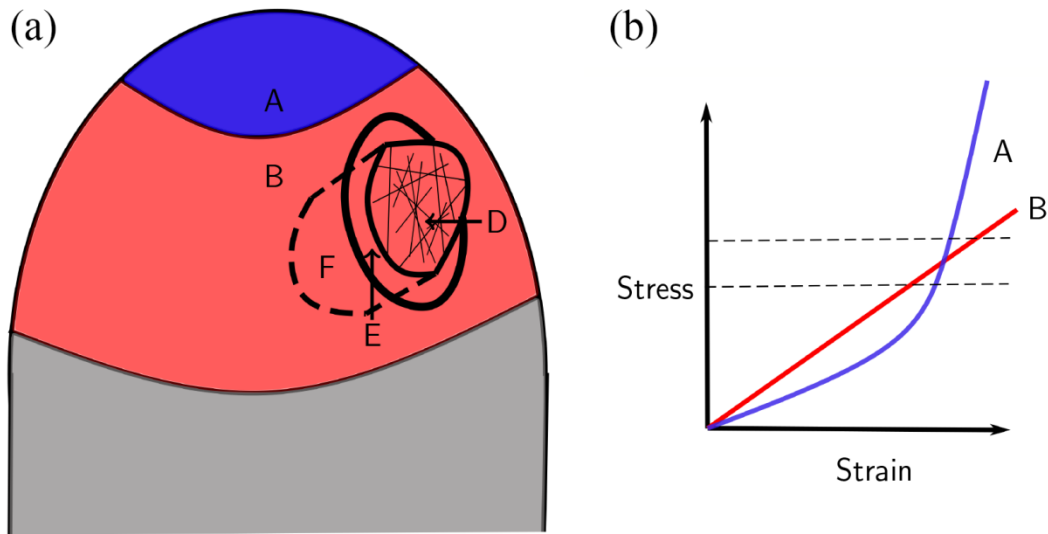
541

542 Further on the topic of SAM, it has been noted that isotropic walls grow slower than
543 anisotropic walls (Armezzani et al. 2018). This confused the understanding of emerging
544 primordia, as their microtubules are in an isotropic setup while still growing faster than the
545 surrounding meristem (Sassi et al. 2014). There also seem to be no change in cellulose
546 deposition to alter the strength of the wall. Therefore there is likely to be some kind of
547 signalling to promote wall loosening (Kierzkowski and Routier-Kierzkowska 2019). Through
548 modelling and experimentation, evidence has been presented that microtubule re-organisation
549 to an isotropic distribution can activate wall loosening genes (and vice versa), allowing organ
550 emergence independently of auxin (Armezzani et al. 2018) (see figure 5). The model makes
551 use of a 2D shell based on Hooke's law, which incorporates fibre orientation and plastic
552 spring growth (figure 4 and 6). The signalling to genes is an essential part, without which
553 isotropic walls in an anisotropic environment are unable to increase growth rates in organ
554 outgrowth. These models all inform us that organ emergence requires not only differential
555 mechanical properties from the tip to the periphery, but also a coupling between genes and
556 the degree of anisotropy.

557

558 The thick, relatively stiff cell walls of the epidermis have been postulated to regulate stem
559 growth via intricate interactions between cells and whole tissues (Baskin and Jensen 2013).
560 It was found that the tissue structure is stabilised by the outer layer's strain stiffening
561 behaviour, without which the tissue could buckle (Vandiver and Goriely 2008). This model
562 was developed by creating a cylindrical model of the stem, consisting of two material layers
563 with different properties. They defined a deformation gradient as the product of a growth
564 tensor, which governs the unrestricted growth of both layers, and an elastic deformation
565 tensor, which couples the layers together. To determine the growth and bending rate of the
566 composite *Arabidopsis* root, a model assigns a yield threshold, wall viscosity and thickness to
567 each individual cell wall segment, varying across cell files (Dyson et al. 2014). This was
568 integrated over the cross section to obtain a tissue-wide Lockhart equation (c.f. eq. (1)).
569 Parametrising with experimental data such as wall thickness and turgor values, they found
570 that the epidermis plays a dominant (6-fold influence) role in regulating extension and
571 described the effectiveness of targeting this layer to cause root bending. Both papers therefore

572 demonstrate the absolute mechanical importance of the epidermis in regulating and
573 stabilising tissues.



574

Figure 5: The requisite shoot apical meristem features for growth and organ emergence. Kierzkowski et al. (2012) demonstrated that in the slow growing apex, region A, there is strain stiffening behaviour and the faster growing periphery, region B, displayed linear behaviour (see (a)). This is depicted in (b) where the dotted line shows the strain at typical levels of turgor. The blue/red line depicts behaviour from region A/B showing the stress increasing rapidly/linearly demonstrating strain hardening in the former. The conditions for organ emergence was modelled by Boudon et al. (2015) who showed reducing the rigidity of the cells in region D allowed for organ emergence site and the creation of a rigid ring of cells in region E around the site can create a distinct bulge emergence. They also note that increased pressure from the bottom layers (region F) does not aid in organ emergence. Armezzani et al. (2018) also predict the necessary isotropic setup of microtubules which signals appropriate wall loosening genes in order for bulge initiation (region D).

575 Stress patterning can be crucial in tissue-wide signalling, as there is increasing evidence that
576 cells can sense these mechanical forces, and that microtubules play a fundamental role in this
577 phenomenon (Hamant and Haswell 2017). Evidence for this claim comes from observations
578 that microtubules align with the stress direction, which allows for the deposition of cellulose
579 to reinforce the cell in the principle direction of stress (Bozorg et al. 2014). Indeed this paper
580 also shows that the microfibril direction is aligned with maximal stress direction and
581 perpendicular to maximal strain direction in the SAM. Using mathematical modelling, one
582 can directly approximate the distribution of stress and then compare it with the organisation
583 of the microtubules (Mirabet et al. 2011). Moreover, by examining stress-feedback and the
584 microtubule patterning at root hair initiation sites, it has been found that circumferential
585 principal stresses around the loosened region lead to radial star configurations of

586 microtubules (Krupinski et al. 2016). More evidence is found in sepals where microtubules
 587 have been shown to align with maximal tension in sepals (Hervieux et al. 2016). At the sepal
 588 tip where growth slows down, microtubules are orientated in a setup that corresponds to fast
 589 anisotropic growth. The model includes a generalised Hooke's law, with a Young's modulus
 590 that increases from the base to the tip, and is solved by finite-element methods. Comparing
 591 this model with experiments leads to the hypothesis that microtubule stress feedback operates
 592 as a shape sensor at the tip and resists further radial expansion.

593 This microtubule function has also been found in the *Arabidopsis* shoot apex, whose shape is
 594 theorised to depend on the microtubule cytoskeleton, which is regulated in turn by the
 595 mechanical stress in a feedback loop (Hamant et al. 2008). The study combines experimental
 596 work, including fluorescent marking of microtubules and tissue imaging, with a shell model
 597 (see figure 4) that includes growing elastic walls elements, proliferation and anisotropy. The
 598 model defines the potential energy in the shell as

$$599 \quad U = \sum_{w \in walls} \frac{k_w}{2} \left(\frac{l_w - l_w^0}{l_w} \right)^2 - \sum_{c \in cells} P_c A_c - \sum_{c \in cells} P_{c,int} V_{c,int}, \quad (4)$$

600 where Σ denotes summation of the wall elements, $w \in walls$ (e.g. segment AC in figure 6) or
 601 cells, $c \in cells$ (e.g. the square ABCD in figure 6). The first term is the contribution of the
 602 wall element elastically stretching, where anisotropy is included in the stiffness k_w of the w^{th}
 603 wall element (this term increases when the w^{th} wall element aligns more closely with a
 604 defined direction of microtubules), which also changes due to stress feedback (microtubule
 605 directions are updated). Plastic spring growth is incorporated by increasing l_w^0 . The second
 606 term in eq. (4) is the force from the internal pressure between cells in the simulated 2D shell
 607 layer (see figure 4), and the third is pressure emerging from the inner tissues including
 608 dependence on both area, A_c and volume, $V_{(c,int)}$. Models are often written in terms of the
 609 energy, because to stretch fibres (elastic deformation), break bonds and/or allow fibres to slip
 610 past each other (viscous/plastic deformation), we require energy. The energy comes from the
 611 action of turgor pressure pushing against the walls in the normal direction. There must then
 612 be a balance between turgor and wall stretching/yielding (figure 6). This is essentially what is

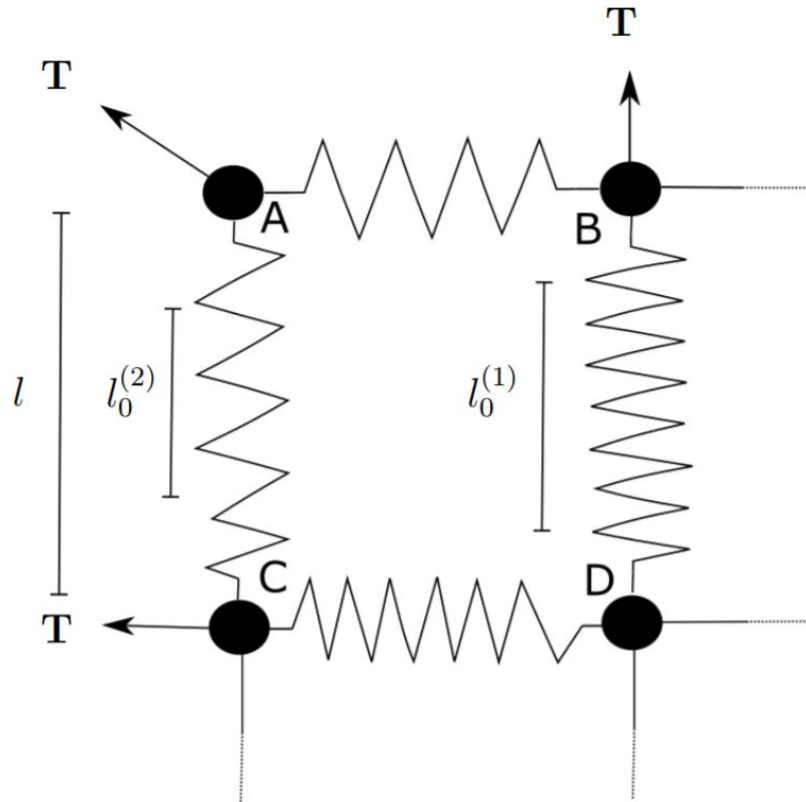


Figure 6: Principles of the vertex element method, plastic spring growth and mechanical energy balance/minimisation. A network of vertices (A,B,C,D) are attached via elements (AB,BD,CD,CA) which are represented as springs. In particular, A, B, C are outside elements with D on the inside. This simplistic system demonstrates the modelling of cell wall extension via plastic spring growth, with dynamically increasing resting lengths $l_0^{(1)}$ and $l_0^{(2)}$ (thus permanently extending the spring). Here the elements AC and BD have the same length l but AC has higher stress because its resting length $l_0^{(2)}$ is shorter than the BD resting length $l_0^{(1)}$ (so AC has undergone larger strain i.e. the difference between the resting length $l_0^{(2)}$ and the actual length l). In other words, given the same stress, BD can stretch more than AC. Plastic spring growth allows the spring to stretch further under the same stress (in practice, models usually impose constant turgor T and hence constant stress, rather than equal l ; the element BD would consequently stretch further than depicted). Energy balance is also at play, as turgor T pushing the outside elements causes the springs to strain (the inside elements, e.g. D, are pushed from all sides equally). The stretch produces an elastic force which opposes the turgor. The position of the vertices are ones that balance the turgor forces and elastic forces.

613 written in eq. (4), where the pressure is balanced with the effect of stretching and plastic
 614 growth. The energy should then be minimised, as physical systems will always favour a state
 615 that requires the least energy (e.g. a ball in a bowl prefers to stay in the bottom where its
 616 gravitational potential energy is minimised). This model is able to replicate observed
 617 microtubule orientations in different experimental scenarios, for example primordium
 618 growth. These studies show that, firstly, microtubules are highly important in stress sensing,
 619 and secondly, they have regulatory effects on the geometry of a tissue.

620

621 The models we have described in this section suggest a fundamental role of mechanical cues
622 in tissue mechanics, provide evidence that the interplay between mechanics and signalling is
623 key to determining observed behaviour, and support the view that genetic regulation alone
624 cannot account for observed phenotypes (Bassel et al. 2014). Questions remain, for example
625 the effect of spatial variations of mechanical properties on cell behaviour, specifically in the
626 SAM, is not yet understood (Truskina and Vernoux 2018). It has also been noted that the
627 feedback loop between microtubules and stress cannot always completely explain how cells
628 develop such a complex geometry in the first place (Kierzkowski and Routier-Kierzkowska
629 2019). Tissue stress origins are also still elusive (Baskin and Jensen 2013). Moreover, the
630 complex relationship between anisotropies and microtubules has not been fully investigated;
631 we will discuss further in section 4.

632

633

634 4 Outlook

635

636 Whilst there have been many success stories where mechanical models have had significant
637 impact on our understanding of plant growth, there are still many exciting future directions
638 for mathematicians and biologists alike to explore.

639

640 The roles and mechanisms of enzyme and protein action in wall loosening have not been
641 fully understood (Cosgrove 2016). Expansins are an important group of non-enzymatic
642 proteins that cause wall stress relaxation, enabling cell wall creep. How they interact with the
643 linkages between microfibrils is unknown. For example, α -expansins have the apparently
644 contradicting effects of inducing creep while maintaining wall strength (Yuan et al. 2001,
645 Wang et al. 2008). Xyloglucan endotransglucosylase/hydrolase (XTH) also affects the cell
646 wall but its action of cutting and rejoining xyloglucans does not necessarily cause an increase
647 in extensibility of the wall (Cosgrove 2016). It also does not seem to affect growth in plants
648 where XTH expression is suppressed (Cosgrove 2005). It could be interesting to explore how
649 expansin/XTH function relates to cell wall structure, as there is the possibility that expansin
650 can cut biomechanical hotspots, that XTH may be ineffective due to a possible inability to
651 access the xyloglucan, or that XTH could control elongation or strengthening by affecting
652 xyloglucan length (Cosgrove 2005, 2014). Endoglucanase expression is also said to have
653 potential to cause wall loosening (Cosgrove 2014). The interactions between different pectin

654 methylesterases (PMEs) are still elusive and it has been proposed that unlocking PME action
655 could help examine pectin's role in the cell wall (Levesque-Tremblay et al. 2015). Models
656 similar to those in section 3.1 might be helpful, where one could examine not just which
657 molecules hold the stress but test possible wall-loosening mechanisms (e.g. expansins
658 targeting hotspots) against experiments.

659

660 Pectins in the cell wall have not been thoroughly investigated, despite their making up over
661 30% of the primary cell walls in most higher plants (Levesque-Tremblay et al. 2015).
662 Although their role has been considered in pollen tubes (Rojas et al. 2011, Fayant et al.
663 2010), in other models their effect has been included as a generic isotropic term. This
664 approach could give an accurate description of pectin's effect (Huang et al. 2015), however it
665 neglects the potential influence of pectin-cellulose interactions, or that de-methylesterified
666 pectin could affect the porosity of cellulose-xyloglucan networks, thereby influencing
667 enzyme action (Cosgrove 2016). Inhibition of PME activity is known to prevent the
668 formation of primordia at the meristem, showing that pectins influence wall extensibility, and
669 that their spatial regulation of methylated and demethylated aids morphogenesis (Höfte et al.
670 2012, Braybrook et al. 2012, Braybrook and Peaucelle 2013) with pectin asymmetry in the
671 hypocotyl epidermis shown to aid anisotropy (Bou Daher et al. 2018). Moreover, even though
672 de-esterified pectin is found in vitro to be stiffer than methyl-esterified pectin, regions of de-
673 esterified pectin can give rise to softer cell walls in the meristem, which is an as-yet
674 unexplained phenomenon (Cosgrove 2016).

675

676 There is evidence that microtubules are highly influential in anisotropy/morphogenesis (see
677 section 3.3), although this relationship is in no way straightforward. It has been found that
678 cellulose fibres in the outer epidermal wall of most stems are orientated axially (Baskin and
679 Jensen 2013), and that anisotropic tissues are not necessarily made up of anisotropic cells
680 (Bou Daher et al. 2018). A related question is how cellulose orientation is decided, because
681 the influence of microtubules on cellulose direction is questionable in some situations
682 (Cosgrove 2014, Bou Daher et al. 2018). Cellulose can also passively re-orientate as the cell
683 grows (Anderson et al. 2010), and although cells may have a net orientation of cellulose
684 fibres, they are deposited in a variety of orientations between lamella layers in the cell walls
685 (Zhang et al. 2016). These features are not often included in models. By incorporating the
686 differences between cells into tissue expansion models, we might be able to identify the

687 possible origins of tissue stress. In addition, models could test different possible mechanisms
688 for cellulose alignment and tissue anisotropy.

689

690 Models which exploit the geometry of growing plant tissues, for example using shell theory,
691 lead to significant reductions in complexity, giving more tractable models and interpretable
692 results. However, some features are often neglected. For example, shell models often assume
693 a straight centreline and thus cannot be used to model steering, twisting or bending.
694 Similarly, emergent anisotropy arising as a tissue-wide phenomenon is often neglected.
695 Indeed, internal layers do contribute to morphogenesis such as the vasculature (Hamant and
696 Haswell 2017). There is therefore a growing need to progress from 2D to 3D models
697 (Kroeger et al. 2008, Fozard et al. 2013).

698

699 Finite-element models can become unstable and less accurate when simulated cell growth
700 causes the elements to increase in length (Fozard et al. 2013). This requires the system to be
701 re-meshed, which can be computationally expensive (Chickarmane et al. 2010). It has also
702 been pointed out that the implementation of finite-element methods in iterations implies that
703 growth occurs in small discrete steps (Fayant et al. 2010). Depending on the number of
704 nodes, this could lead to subtle shape changes, even though a fine mesh density could
705 possibly ensure the errors are small.

706

707

708 5 Summary

709

710 In this review we have demonstrated that mathematical models can help unravel mysteries of
711 how the cell wall structure allows controlled growth, what causes intricate tissue
712 morphologies and how stress feedback works across whole tissues. For mathematicians, plant
713 biomechanics is a truly exciting field in which great opportunities beckon, with numerous
714 fascinating questions and opportunities for impactful work.

715

716 Some of the best models have resulted from multidisciplinary collaborations between
717 mathematicians and biologists, which allow modelling and experimentation to be adapted to
718 each other in real time. It is therefore vital for the progress of the field that mathematicians
719 and biologists work together to produce models which are experimentally verifiable, can

720 explain biological phenomena mechanistically, and can raise important new questions about
721 the elusive nature of plant biology.

722

723

724 6 Acknowledgments

725

726 We would like to thank Joanna Chustecki, James Tyrrell and Clare Ziegler for their helpful
727 inputs. RJD and ETS thank EPSRC for funding via grants EP/M0015X/1 and EP/N509590/1.
728 ETS thanks the QJMAM fund for facilitating attendance at the Plant Biomechanics
729 Conference 2018. JL thanks the University of Birmingham for Postdoctoral Fellowship
730 funding. We would also like to thank the reviewers for their constructive feedback.

731

732 REFERENCES

733 **Ali O, Mirabet V, Godin C, Traas J.** 2014. Physical models of plant development. Annual
734 Review of Cell and Developmental Biology **30**, 59–78.

735 **Ali O, Traas J.** 2016. Force-driven polymerization and turgor-induced wall expansion.
736 Trends in Plant Science **21**, 398–409.

737 **Anderson CT, Carroll A, Akhmetova L, Somerville C.** 2010. Real-time imaging of
738 cellulose reorientation during cell wall expansion in *Arabidopsis* roots. Plant Physiology **152**,
739 787–796.

740 **Anderson P.** 1972. More is different. Science **177**, 393–396.

741 **Arfken G, Weber H.** 1995. Mathematical Methods for Physicists. Ch. 2, pp. 126-154, 4th
742 edn, Academic Press, London.

743 **Armezzani A, Abad U, Ali O, et al.** 2018. Transcriptional induction of cell wall remodelling
744 genes is coupled to microtubule-driven growth isotropy at the shoot apex in *Arabidopsis*.
745 Development doi: 10.1242/dev.162255

746 **Astarita G, Marrucci G.** 1974. Principles of Non-Newtonian Fluid Mechanics. Ch. 1, pp. 1-
747 41, McGraw-Hill, Maidenhead.

748 **Barbacci, A, Lahaye M, Magnenet.** 2013. Another brick in the cell wall: biosynthesis
749 dependent growth model, PLOS ONE doi: 10.1371/journal.pone.0074400

750 **Baskin TI.** 2001. On the alignment of cellulose microfibrils by cortical microtubules: a
751 review and a model. Protoplasma **215**, 150–171.

752 **Baskin TI.** 2005. Anisotropic expansion of the plant cell wall. *Annual Review of Cell and*
753 *Developmental Biology* **21**, 203–222.

754 **Baskin TI, Jensen OE.** 2013. On the role of stress anisotropy in the growth of stems. *Journal*
755 *of Experimental Botany* **64**, 4697–4707.

756 **Bassel GW, Stamm P, Mosca G, de Reuille PB, Gibbs DJ, Winter R, Janka A,**
757 **Holdsworth MJ, Smith RS.** 2014. Mechanical constraints imposed by 3d cellular geometry
758 and arrangement modulate growth patterns in the *Arabidopsis* embryo. *Proceedings of the*
759 *National Academy of Sciences* doi: 10.1073/pnas.1404616111

760 **Beauzamy L, Louveaux M, Hamant O, Boudaoud A.** 2015. Mechanically, the shoot apical
761 meristem of *Arabidopsis* behaves like a shell inflated by a pressure of about 1 mpa. *Frontiers*
762 *in Plant Science* doi: 10.3389/fpls.2015.01038

763 **Beauzamy L, Nakayama N, Boudaoud A.** 2014. Flowers under pressure: ins and outs of
764 turgor regulation in development. *Annals of Botany* **114**, 1517–1533.

765 **Bidhendi AJ, Geitmann A.** 2018. finite element modeling of shape changes in plant cells.
766 *Plant Physiology* doi: 10.1104/pp.17.01684

767 **Bidhendi A, Geitmann A.** 2019. Geometrical details matter for mechanical modeling of cell
768 morphogenesis. *Developmental Cell*, in press.

769 **Bidhendi A, Geitmann A.** 2019. Methods to quantify primary plant cell wall mechanics.
770 *Journal of Experimental Botany*, in press.

771 **Bidhendi, AJ, Altartouri B, Gosselin F, Geitmann A.** 2019. Mechanical stress initiates and
772 sustains the morphogenesis of wavy leaf epidermal cells. *bioRxiv* doi: doi:
773 <https://doi.org/10.1101/563403>

774 **Bird R, Armstrong R, Hassager O.** 1987. *Dynamics of Polymeric Liquids. Volume 1: Fluid*
775 *Mechanics*, Ch. 4, pp. 169-236, 2nd edn, John Wiley and Sons, New York.

776 **Boudon F, Chopard J, Ali O, Gilles B, Hamant O, Boudaoud A, Traas J, Godin C.** 2015.
777 A computational framework for 3d mechanical modeling of plant morphogenesis with
778 cellular resolution. *PLOS Computational Biology* doi: 10.1371/journal.pcbi.1003950

779 **Bove J, Vaillancourt B, Kroeger J, Hepler PK, Wiseman PW, Geitmann A.** 2008.
780 Magnitude and direction of vesicle dynamics in growing pollen tubes using spatiotemporal
781 image correlation spectroscopy and fluorescence recovery after photobleaching. *Plant*
782 *Physiology* **147**, 1646–1658.

783 **Bozorg B, Krupinski P, Jönsson H.** 2014. Stress and strain provide positional and
784 directional cues in development. *PLOS Computational Biology* doi:
785 10.1371/journal.pcbi.1003410

786 **Braybrook SA, Hofte H, Peaucelle A.** 2012. Probing the mechanical contributions of the
787 pectin matrix: insights for cell growth. *Plant Signaling & Behavior* **7**, 1037–1041.

788 **Braybrook SA, Peaucelle A.** 2013. Mechano-chemical aspects of organ formation in
789 *Arabidopsis thaliana*: the relationship between auxin and pectin. *PLOS ONE* doi:
790 10.1371/journal.pone.0057813

791 **Bruce DM.** 2003. Mathematical modelling of the cellular mechanics of plants. *Philosophical*
792 *Transactions of the Royal Society of London B: Biological Sciences* **358**, 1437–1444.

793 **Brujan EA.** 2011. Cavitation in Non-Newtonian Fluids: with Biomedical and Bioengineering
794 Applications. Ch. 1, pp. 1-43, Springer, Heidelberg.

795 **Cameron C, Geitmann A.** 2018. Cell mechanics of pollen tube growth. *Current Opinion in*
796 *Genetics & Development* **51**, 11–17.

797 **Chebli Y, Geitmann A.** 2007. Mechanical principles governing pollen tube growth.
798 *Functional Plant Science and Biotechnology* **1**, 232–245.

799 **Chickarmane V, Roeder AH, Tarr PT, Cunha A, Tobin C, Meyerowitz EM.** 2010.
800 Computational morphodynamics: a modeling framework to understand plant growth. *Annual*
801 *Review of Plant Biology* **61**, 65–87.

802 **Cosgrove DJ.** 1993. How do plant cell wall extend? *Plant Physiology* **102**, 1–6.

803 **Cosgrove DJ.** 2005. Growth of the plant cell wall. *Nature Reviews Molecular Cell Biology*
804 **6**, 850–861.

805 **Cosgrove DJ.** 2014. Re-constructing our models of cellulose and primary cell wall assembly.
806 *Current Opinion in Plant Biology* **22**, 122–131.

807 **Cosgrove DJ.** 2016. Catalysts of plant cell wall loosening. *F1000Research* doi:
808 10.12688/f1000research.7180.1

809 **Bou Daher F, Chen Y, Bozorg B, Clough JH, Jönsson H, Braybrook SA.** 2018.
810 Anisotropic growth is achieved through the additive mechanical effect of material anisotropy
811 and elastic asymmetry. *eLife* doi: 10.7554/eLife.38161

812 **de Reuille PB, Routier-Kierzkowska AL, Kierzkowski D, et al.** 2015. MorphoGraphX: a
813 platform for quantifying morphogenesis in 4d. *eLife* doi: 10.7554/eLife.05864

814 **Dumais J.** 2007, Can mechanics control pattern formation in plants? *Current Opinion in*
815 *Plant Biology* **10**, 58–62.

816 **Dill E.** 2007. *Continuum Mechanics: Elasticity, Plasticity, Viscoelasticity.* Ch. 5, p. 213 ff.,
817 CRC Press, Boca Raton, FL.

818 **Dumais J, Shaw SL, Steele CR, Long SR, Ray PM.** 2006. An anisotropic-viscoplastic
819 model of plant cell morphogenesis by tip growth. *The International Journal of Developmental*
820 *Biology* **50**, 209–222.

821 **Dupuy L, Mackenzie J, Rudge T, Haseloff J.** 2007. A system for modelling cell–cell
822 interactions during plant morphogenesis. *Annals of Botany* **101**, 1255–1265.

823 **Dyson RJ, Band L, Jensen O.** 2012. A model of crosslink kinetics in the expanding plant
824 cell wall: yield stress and enzyme action. *Journal of Theoretical Biology* **307**, 125–136.

825 **Dyson RJ, Jensen O.** 2010. A fibre-reinforced fluid model of anisotropic plant cell growth.
826 *Journal of Fluid Mechanics* **655**, 472–503.

827 **Dyson RJ, Vizcay-Barrena G, Band LR et al.** 2014. Mechanical modelling quantifies the
828 functional importance of outer tissue layers during root elongation and bending. *New*
829 *Phytologist* **202**, 1212–1222.

830 **Edelstein-Keshet L.** 2005. *Mathematical Models in Biology*. Ch. 4, pp. 126-128, SIAM,
831 Philadelphia, PA.

832 **Elman H, Silvester D, Wathen A.** 2005. *Finite Elements and Fast Iterative Solvers: with*
833 *Applications in Incompressible Fluid Dynamics*. Ch. 7, p 313 ff. and Ch. 8, p 341 ff., OUP,
834 Oxford.

835 **Eringen A.** 1980. *Mechanics of Continua.*, Ch. 2, pp. 89-91, 2nd edn, Robert E. Krieger,
836 Melbourne, FL.

837 **Evans G, Blackledge J, Yardley P.** 2000. *Numerical Methods for Partial Differential*
838 *Equations*. Ch. 6, p. 165 ff., Springer-Verlag, London.

839 **Fawcett TW, Higginson AD.** 2012. Heavy use of equations impedes communication among
840 biologists, *Proceedings of the National Academy of Sciences* **109**, 11735–11739.

841 **Fayant P, Girlanda O, Chebli Y, Aubin C-É, Villemure I, Geitmann A.** 2010. Finite
842 element model of polar growth in pollen tubes. *The Plant Cell* **22**, 2579–2593.

843 **Fozard JA, Lucas M, King JR, Jensen OE.** 2013. Vertex-element models for anisotropic growth
844 of elongated plant organs. *Frontiers in Plant Science* doi: 10.3389/fpls.2013.00233

845 **Geitmann A, Dyson R.** 2013. Modeling of the primary plant cell wall in the context of plant
846 development. *Cell Biology* doi: https://doi.org/10.1007/978-1-4614-7881-2_8-1

847 **Geitmann A, Ortega JK.** 2009. Mechanics and modeling of plant cell growth. *Trends in*
848 *Plant Science* **14**, 467–478.

849 **Goodier J, Hodge P.** 1958. *Elasticity and Plasticity*. John Wiley and Sons, New York.

850 **Hamant O, Haswell ES.** 2017. Life behind the wall: sensing mechanical cues in plants.
851 *BMC biology* doi: 10.1186/s12915-017-0403-5

852 **Hamant O, Heisler MG, Jönsson H et al.** 2008. Developmental patterning by mechanical
853 signals in *Arabidopsis*. *Science* **322**, 1650–1655.

854 **Hervieux N, Dumond M, Sapala A, Routier-Kierzkowska A-L, Kierzkowski D, Roeder**
855 **AHK, Smith RS, Boudaoud A, Hamant O.** A Mechanical Feedback Restricts Sepal Growth
856 and Shape in *Arabidopsis*. *Current Biology* **26**, 1019-1028.

857 **Huang R, Becker AA and Jones IA.** 2015. A finite strain fibre-reinforced viscoelasto-
858 viscoplastic model of plant cell wall growth. *Journal of Engineering Mathematics* **95**, 121–
859 154.

860 **Jarvis MC.** 2009. Plant cell walls: supramolecular assembly, signalling and stress. *Structural*
861 *Chemistry* **20**, 245–253.

862 **Kevorkian J.** 2000. *Partial Differential Equations: Analytical Solution Techniques*. Ch.8, pp.
863 525-576, 2nd edn, Springer-Verlag, New York.

864 **Kierzkowski D, Nakayama N, Routier-Kierzkowska A-L, Weber A, Bayer E,**
865 **Schoreret, M, Reinhardt D, Kuhlemeier C, Smith RS.** 2012. Elastic domains regulate
866 growth and organogenesis in the plant shoot apical meristem. *Science* **335**, 1096–1099.

867 **Kierzkowsk D, Routier-Kierzkowska A-L.** 2019. Cellular basis of growth in plants:
868 geometry matters. *Current Opinion in Plant Biology* **47**, 56–63.

869 **Kroeger JH, Geitmann A.** 2012. Pollen tube growth: getting a grip on cell biology through
870 modelling. *Mechanics Research Communications* **42**, 32–39.

871 **Kroeger JH, Geitmann A, Grant M.** 2008. Model for calcium dependent oscillatory growth
872 in pollen tubes. *Journal of Theoretical Biology* **253**, 363–374.

873 **Krupinski P, Bozorg B, Larsson A, Pietra S, Grebe M, Jönsson H.** 2016. A model
874 analysis of mechanisms for radial microtubular patterns at root hair initiation sites. *Frontiers*
875 *in Plant Science* doi: 10.3389/fpls.2016.01560

876 **Levesque-Tremblay G, Pelloux J, Braybrook SA, Müller K.** 2015. Tuning of pectin
877 methylesterification: consequences for cell wall biomechanics and development. *Planta* **242**,
878 791–811.

879 **Lockhart JA.** 1965. An analysis of irreversible plant cell elongation. *Journal of Theoretical*
880 *Biology* **8**, 264–275.

881 **Majda M, Grones P, Sintorn I-M et al.** 2017. Mechanochemical polarization of contiguous
882 cell walls shapes plant pavement cells. *Developmental Cell* **43**, 290–304.

883 **Mattheij R, Rienstra S, ten Thije Boonkkamp J.** 2005. *Partial Differential Equations:*
884 *Modeling, Analysis, Computation*. Ch. 2, pp. 13-29 and Ch 16, p 501 ff., SIAM,
885 Philadelphia, PA.

886 **Mirabet V, Das P, Boudaoud A, Hamant O.** 2011. The role of mechanical forces in plant
887 morphogenesis. *Annual Review of Plant Biology* **62**, 365–385.

888 **Nili A, Yi H, Crespi VH, Puri VM.** 2015. Examination of biological hotspot hypothesis of
889 primary cell wall using a computational cell wall network model. *Cellulose* **22**, 1027–1038.

890 **Ogden R.** 2013. *Non-Linear Elastic Deformations*, Ch. 4, pp. 204-222, Dover, Mineola, NY.

891 **O'Malley R.** 2014. *Historical Developments in Singular Perturbations*. Ch. 2, pp. 27-31,
892 Springer, Cham, Switzerland.

893 **Paolucci S.** 2016. *Continuum Mechanics and Thermodynamics of Matter*. Ch. 5, pp. 191-
894 194, CUP, Cambridge.

895 **Park YB, Cosgrove DJ.** 2015. Xyloglucan and its interactions with other components of the
896 growing cell wall. *Plant and Cell Physiology* **56**, 180–194.

897 **Parker D.** 2003. *Fields, Flows and Waves: An Introduction to Continuum Models*. Ch. 6, p.
898 101 ff., Springer-Verlag, London.

899 **Peaucelle A, Braybrook S, Höfte H.** 2012. Cell wall mechanics and growth control in
900 plants: the role of pectins revisited. *Frontiers in Plant Science* doi: 10.3389/fpls.2012.00121.

901 **Pietruszka M.** 2011. Solutions for a local equation of anisotropic plant cell growth: an
902 analytical study of expansin activity. *Journal of The Royal Society Interface* **8**, 975–987.

903 **Prusinkiewicz P.** 2004. Modeling plant growth and development. *Current Opinion in Plant Biology*
904 **7**, 79–83.

905 **Ptashnyk M, Seguin B.** 2016. The impact of microfibril orientations on the biomechanics of
906 plant cell walls and tissues. *Bulletin of Mathematical Biology* **78**, 2135–2164.

907 **Renteln P.** 2014. *Manifolds, Tensors, and Forms: An Introduction for Mathematicians and*
908 *Physicists*. Ch. 2, pp. 30-48, CUP, Cambridge.

909 **Rojas ER, Hotton S, Dumais J.** 2011. Chemically mediated mechanical expansion of the
910 pollen tube cell wall. *Biophysical Journal* **101**, 1844–1853.

911 **Sampathkumar A, Krupinski P, Wightman R, Milani P, Berquand A, Boudaoud A,**
912 **Hamant O, Jönsson H, Meyerowitz EM.** 2014. Subcellular and supracellular mechanical
913 stress prescribes cytoskeleton behavior in *Arabidopsis* cotyledon pavement cells, *eLife*
914 doi:10.7554/eLife.01967.

915 **Sandler S.** 1999, *Chemical and Engineering Thermodynamics*, Ch. 3, pp. 89-97, 3rd edn, John
916 Wiley and Sons, New York.

917 **Sapala A, Runions A, Routier-Kierzkowska A-L et al.** 2018. Why plants make puzzle
918 cells, and how their shape emerges. *eLife* doi: 10.7554/eLife.32794

919 **Sapala A, Runions A, Smith RS.** 2019. Mechanics, geometry and genetics of epidermal cell
920 shape regulation: different pieces of the same puzzle. *Current Opinion in Plant Biology* **47**,
921 1–8.

922 **Sassi M, Ali O, Boudon F et al.** 2014, An auxin-mediated shift toward growth isotropy
923 promotes organ formation at the shoot meristem in *Arabidopsis*, *Current Biology* **24**, 2335–
924 2342.

925 **Savaldi-Goldstein S, Peto C, Chory J.** 2007, The epidermis both drives and restricts plant
926 shoot growth. *Nature* **446**, 199–202.

927 **Scheller HV, Ulvskov P.** 2010. Hemicelluloses, *Annual Review of Plant Biology* **61**, 263–
928 289.

929 **Soyars CL, James SR, Nimchuk ZL.** 2016, Ready, aim, shoot: stem cell regulation of the
930 shoot apical meristem, *Current Opinion in Plant Biology* **29**, 163–168.

931 **Spencer A.** 2004. *Continuum Mechanics*, Ch. 5, pp. 44-59; Ch. 8, pp. 110-116; and Ch. 10,
932 pp. 136-142, Dover, Mineola, NY.

933 **Steinrück H.** 2010. Introduction to matched asymptotic methods, *Asymptotic Methods in*
934 *Fluid Mechanics: Survey and Recent Advances (CISM Courses and Lecture, vol. 523)*,
935 CISM, Udine, Italy, pp. 1–22.

936 **Truskina J, Vernoux T.** 2018. The growth of a stable stationary structure: coordinating cell
937 behavior and patterning at the shoot apical meristem, *Current Opinion in Plant Biology* **41**,
938 83–88.

939 **Vandiver R, Goriely A.** 2008. Tissue tension and axial growth of cylindrical structures in
940 plants and elastic tissues. *Europhysics Letters* doi: 10.1209/0295-5075/84/58004

941 **Veytsman BA, Cosgrove DJ.** 1998. A model of cell wall expansion based on
942 thermodynamics of polymer networks. *Biophysical Journal* **75**, 2240–2250.

943 **Vofély RV, Gallagher J, Pisano GD, Bartlett M, Braybrook SA.** 2018. Of puzzles and
944 pavements: a quantitative exploration of leaf epidermal cell shape. *New Phytologist* doi:
945 10.1111/nph.15461

946 **Wang C, Wang L, McQueen-Mason S, Pritchard J, Thomas C.** 2008. pH and expansin
947 action on single suspension-cultured tomato (*Lycopersicon esculentum*) cells. *Journal of Plant*
948 *Research* **121**, 527–534.

949 **Yi H, Puri VM.** 2012. Architecture-based multiscale computational modeling of plant cell
950 wall mechanics to examine the hydrogen-bonding hypothesis of cell wall network structure
951 model. *Plant Physiology* **160**, 1281–1292.

- 952 **Yuan S, Wu Y, Cosgrove DJ.** 2001. A fungal endoglucanase with plant cell wall extension
953 activity, *Plant Physiology* **127**, 324–333.
- 954 **Zhang T, Zheng Y, Cosgrove DJ.** 2016. Spatial organization of cellulose microfibrils and
955 matrix polysaccharides in primary plant cell walls as imaged by multichannel atomic force
956 microscopy. *The Plant Journal* **85**, 179–192.
- 957 **Zheng Y, Wang X, Chen Y, Wagner E, Cosgrove DJ.** 2018. Xyloglucan in the primary cell
958 wall: assessment by feSEM, selective enzyme digestions and nanogold affinity tags. *The Plant*
959 *Journal* **93**, 211–226.